Cambridge Part III Maths

Lent 2020

Fluid Dynamics of the Solid Earth

based on a course given by
Dr. Jerome Neufeld

written up by
Charles Powell

Contents

Lecture 1
21/01/21

1 Introduction

The course will use the wealth of observations of the solid Earth to motivate mathematical models of the physical processes governing its evolution. The dynamic evolution is governed by a rich variety of physical processes occuring on a wide range of length and time scales.

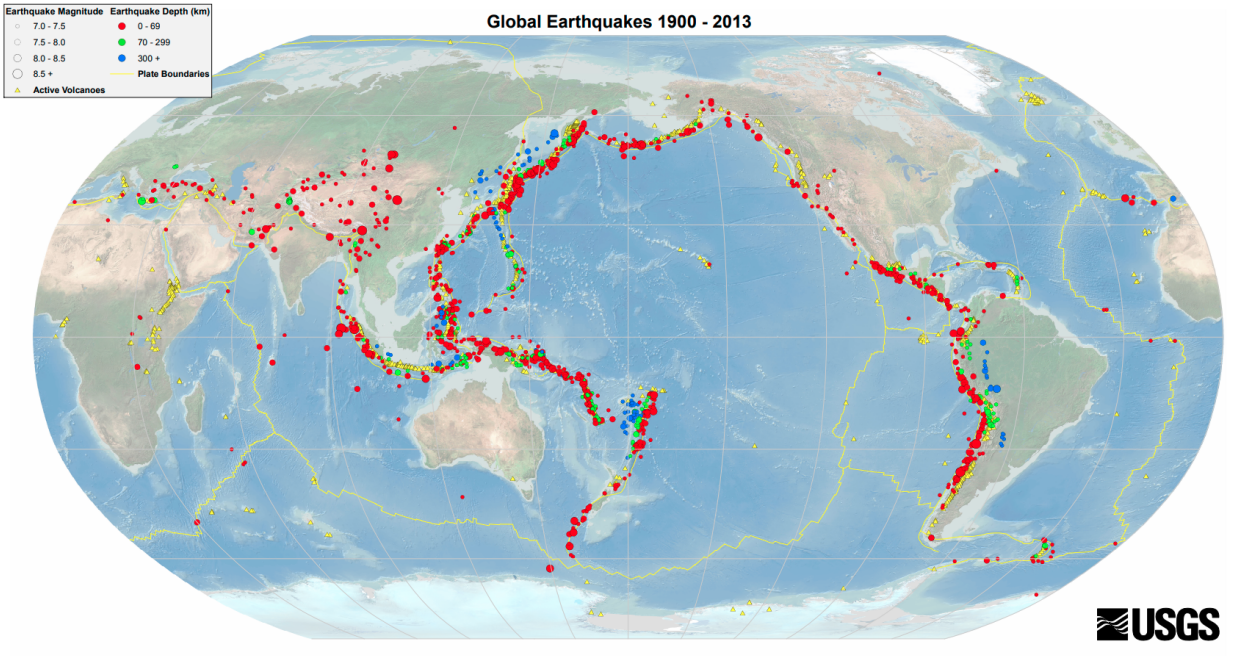

Figure 1: Map of global earthquakes, visibly localised to tectonic plate boundaries.

- The Earth's core is formed by the solidifcation of a mixture of molten iron and various light elements, a process which drives predominantly compositional convection in the liquid outer core, thus producing the geodynamo responsible for the Earth's magnetic field.
- On million year timescales, the solid mantle convects, and as it upwells to the surface it partially melts leading to the volcanism.
- At the surface, convection drives the motion of brittle plates which are responsible for the Earth's topography as can be felt and imaged through the seismic record (figure 1)
- In the Earth's surface, fluids flow through porous rocks, for example groundwater aquifers which feed streams and rivers which erode the solid surface.
- On the Earth's surface, similar physical processes of viscous and elastic deformation coupled to phase changes govern the evolution of the Earth's cryosphere, from the solidification of sea ice to the flow of glacial ice over land and ice shelves over the ocean.

Predominantly, the mathematics is of slow viscous flows. Topics include the onset and scaling of convection, the coupling of fluid motions with changes of phase at a boundary, the thermodynamic and mechanical evolution of multicomponent or multiphase systems, the coupling of fluid flow and elastic flexure or deformation, and the flow of fluids through porous materials.

2 Plate cooling

Here we consider a half-space cooling model of the oceanic lithosphere (oceanic plates). The bottom surface of Earth's oceans, particularly clear in the Atlantic ocean, has a large scale structure in which the middle of the ocean (the *mid-ocean ridge*) is shallower than regions closer to the continents. The mid-ocean ridge forms as a result of separating tectonic plates. We know that the plates move apart here due to magnetic anomalies forming 'stripes' of alternating polarity. The

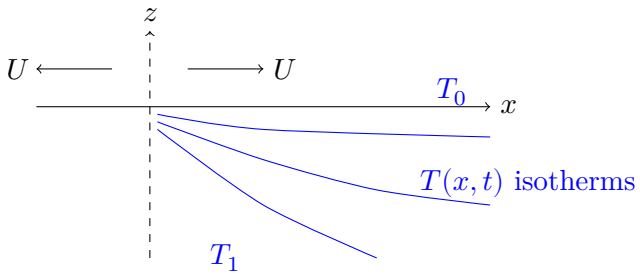

Figure 2: Schematic diagram of mid-ocean ridge spreading and mantle temperature isotherms.

quasi-periodic flipping of the Earth's magnetic polarity allows dating of the stripes. The plates are driven apart by convection of the Earth's mantle.

2.1 Thermal problem

We wish to form a model describing the depth of the ocean floor near mid-ocean ridges. First we estimate the temperature field. Consider an idealised model with a flat surface (for now), observed plate spreading rate U, surface temperature T_0, deep mantle temperature T_1. The temperature field is described by the advection-diffusion equation

$$\rho c_p \left(\frac{\partial T}{\partial t} + \boldsymbol{u} \cdot \nabla T \right) = \nabla \cdot (k \nabla T)$$

where c_p is specific heat capacity, k is thermal conductivity, ρ is density, all assumed constant. For simplicity, we combine these constants into the thermal diffusivity $\kappa = k/\rho c_p$. Then

$$\frac{\partial T}{\partial t} + \boldsymbol{u} \cdot \nabla T = \kappa \nabla^2 T$$

We wish to find the steady state profile with $\partial_t = 0, \boldsymbol{u} = U\hat{\boldsymbol{x}}$ where U is constant. Note that far from the ridge axis, the thickness of the plate is much smaller than the extent of the plate. Hence in terms of scalings, $z \ll x$ and we may neglect the ∂_x^2 component of ∇^2. We have

$$U \frac{\partial T}{\partial x} = \kappa \left(\frac{\partial^2 T}{\partial x^2} + \frac{\partial^2 T}{\partial z^2} \right) \approx \kappa \frac{\partial^2 T}{\partial z^2} \tag{1}$$

The scaling given by this equation is $U\Delta T/x \sim \kappa \Delta T/z^2$ where $\Delta T = T_1 - T_0$ is the natural temperature scale. There is no natural lengthscale, so we use that given by the advection-diffusion equation:

$$z \sim \sqrt{\frac{\kappa x}{U}}$$

We can proceed by finding a self-similar solution with similarity variable

$$\eta = \frac{z}{2\sqrt{\frac{\kappa x}{U}}}$$

and seek solutions of the form

$$\theta = \frac{T - T_0}{T_1 - T_0} = \theta(\eta)$$

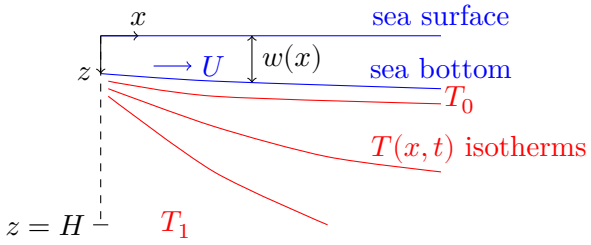

Figure 3: Schematic diagram of ocean depth and crust temperature surfaces.

Using the variables η, θ, (1) becomes

$$-U\Delta T\frac{\eta}{2x}\theta_\eta = \frac{\kappa\Delta T}{4\frac{\kappa x}{U}}\theta_{\eta\eta}$$
$$\implies \theta_{\eta\eta} + 2\eta\theta_\eta = 0$$

We can integrate directly to get $\theta_\eta = ae^{-\eta^2}$, which gives

$$\theta = b + a\int_0^\eta e^{-y^2}\,\mathrm{d}y$$

The boundary conditions are $\theta(0) = 1$ and $\theta(\infty) = 1$ based on the definitions of T_0 and T_1. The thermal structure away from the ridge is then

$$T = T_0 + (T_1 - T_0)\,\mathrm{erf}\left(\frac{z}{2\sqrt{\frac{\kappa x}{U}}}\right) \tag{2}$$

where the error function erf and its complement erfc are defined by

$$\mathrm{erf}(x) = \frac{2}{\sqrt{\pi}}\int_0^x e^{-y^2}\,\mathrm{d}y$$
$$\mathrm{erfc}(x) = 1 - \mathrm{erf}(x)$$

2.2 Ocean depth away from mid-ocean ridge

We now consider the depth of the ocean following from the temperature field derived above. We choose axes with z increasing downwards, placing the sea surface at $z = 0$ and the 'bottom' of the mantle at $z = H$. The coordinate x increases away from the mid-ocean ridge, with ocean depth $w(x)$ at a given x.
First, consider *isostacy*: Archimedean buoyancy applied to Earth's crust. This indicates the depth at which an object/fluid parcel of some density lies in a fluid of different density.

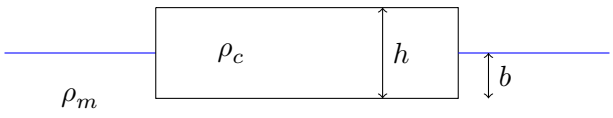

Denoting the density of the crust and mantle as ρ_c, ρ_m respectively, the crust of thicknes h sits at a depth b in the mantle. Hydrostatic balance gives $\rho_c gh = \rho_m gb$. Equivalently, we can consider a force balance between the weight of the curst and the buoyancy force:

$$\rho_c(h - b)g = (\rho_m - \rho_c)gb$$

Within the oceanic lithosphere we have a denssity field

$$\rho = \rho_m \left(1 - \alpha(T - T_1)\right)$$

where $T = T(x, z)$ is the thermal model derived above, given by (2). Isostatic balance gives the following, which balances water weight, mantle weight, with water and mantle buoyancy. The ocean density is denoted by ρ_w.

$$\begin{aligned}
\rho_w w_0 + \rho_m (H - w_0) &= \rho_w w(x) + \int_w^H \rho(T)\,\mathrm{d}z \\
&= \rho_w w + \rho_m (H - w) - \rho_m \alpha \int_w^H (T - T_1)\,\mathrm{d}z \\
\implies (\rho_m - \rho_w)(w - w_0) &= -\rho_m \alpha \int_w^H (T - T_1)\,\mathrm{d}z \\
&\approx -\rho_m \alpha (T_1 - T_0) \int_0^\infty \operatorname{erfc}(\eta) \cdot 2\sqrt{\frac{\kappa x}{U}}\,\mathrm{d}\eta
\end{aligned}$$

where the last approximate equality follows from taking $w \to 0$ and $H \to \infty$, approximating the fact the mantle is much deeper than the ocean. The ocean depth is therefore

$$w - w_0 = \frac{\rho_m}{\rho_m - \rho_w} \alpha (T_1 - T_0) \frac{2}{\sqrt{\pi}} \left(\frac{\kappa x}{U}\right)^{1/2}$$

This model fits the data well near to the mid-ocean ridge, with crust age up to 75 million years. However, away from the ridge, the model breaks down as w tends to a constant as $x \to \infty$. The breakdown of the model is due to convection: the infinite depth curst approximation breaks down and convection dynamics become important.

3 Natural convection

Natural convection arises in flows driven by density differences in a gravitational field, e.g. due to temperature or composition.

3.1 Static stability

Consider the case of no fluid motion $\boldsymbol{u} = 0$ and initial stratification $\rho = \rho_0(1 + \beta z)$. If $\beta < 0$, the dynamics are statically stable. If $\beta > 0$, the dynamics are statically unstable but dynamically could be stable.

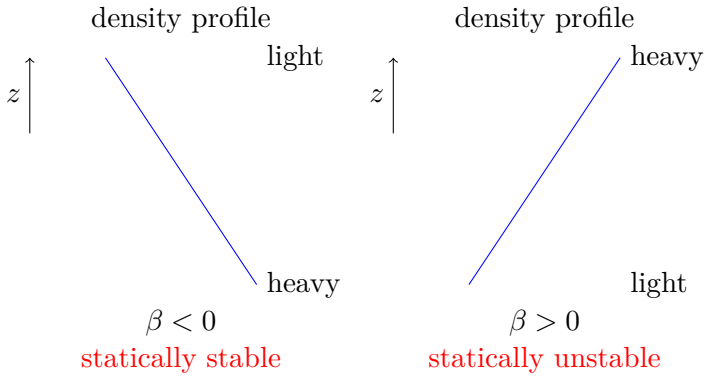

Scaling analysis. Consider a fluid parcel of characteristic size l in unstable density profile $\rho = \rho_0(1+\beta z), \beta > 0$. Suppose the parcel moves up a distance h in time τ.

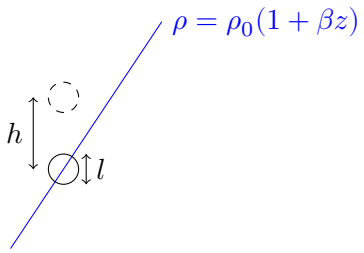

The rise of the fluid parcel relasess potential energy E which scales as

$$E \sim (\Delta\rho l^3)gh \sim (\rho_0 \beta h l^3)gh \sim \rho_0 \beta g h^2 l^3$$

The timescale for the rising motion is limited by diffusion of buoyancy (i.e. diffusion of temperature in this case) so $\tau \sim l^2/\kappa$ where κ is thermal diffusivity. Viscous dissipation over timescale τ scales as the shear stress times the distance travelled:

$$\mathcal{D} \sim \frac{\mu U}{l} l^2 h \sim \mu \frac{h/\tau}{l} l^2 h \sim \frac{\mu\kappa h^2}{l}$$

Instability arises if $E \gtrapprox \mathcal{D}$, which we can write as

$$\rho_0 \beta g h^2 l^3 \gtrapprox \frac{\mu\kappa h^2}{l}$$

Define the *Rayleigh number*

$$\mathrm{Ra} = \frac{\rho_0 \beta g l^4}{\kappa\mu}$$

which quantifies the ratio of timescales of thermal transport via diffusion versus via convection. If Ra is large, the flow is more turbulent. There is instability if $\mathrm{Ra} \gtrapprox \mathcal{O}(1)$.

3.2 Onset of convection

Consider a fluid of depth h between $z = 0$ and $z = h$ with density profile $\rho(z)$ and temperature difference ΔT across the depth.

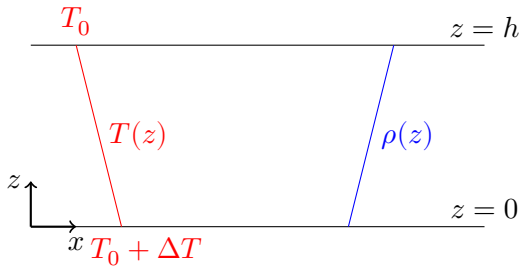

The governing equations are conservation of mass (3), conservation of momentum (4), and conservation of energy (5).

$$\nabla \cdot \boldsymbol{u} = 0 \tag{3}$$

$$\rho\left(\frac{\partial \boldsymbol{u}}{\partial t} + \boldsymbol{u}\cdot\nabla\boldsymbol{u}\right) = -\nabla p + \mu\nabla^2\boldsymbol{u} - \rho g\hat{\boldsymbol{z}} \tag{4}$$

$$\rho c_p\left(\frac{\partial T}{\partial t} + \boldsymbol{u}\cdot\nabla T\right) = \nabla\cdot(k\nabla T) \tag{5}$$

For steady solutions with $\boldsymbol{u} = 0$ and $\partial_t = 0$ we find

$$\begin{aligned} T &= T_0 + \Delta T\left(1 - \frac{z}{h}\right) \\ \frac{\partial p}{\partial x} = \frac{\partial p}{\partial y} &= 0 \\ \frac{\partial p}{\partial z} &= -\rho_0 g\left(1 - \alpha(T - T_0)\right) \end{aligned}$$

We assess the stability by examining small perturbations to a steady base state:

$$\begin{aligned} \boldsymbol{u} &= 0 + \boldsymbol{u}'(\boldsymbol{x}, t) \\ T &= T_0 + \Delta T\left(1 - \frac{z}{h}\right) + T'(\boldsymbol{x}, t) \\ p &= p_0(z) + p'(\boldsymbol{x}, t) \end{aligned}$$

The linearied perturbation equations are thus

$$\begin{aligned} \nabla \cdot \boldsymbol{u}' &= 0 \\ \rho_0 \frac{\partial \boldsymbol{u}'}{\partial t} &= -\nabla p' + \mu \nabla^2 \boldsymbol{u}' + \rho_0 g \alpha T' \hat{\boldsymbol{z}} \\ \frac{\partial T'}{\partial t} - \frac{\Delta T}{h} w' &= \kappa \nabla^2 T' \end{aligned}$$

Non-dimensionalising. We wish to non-dimensionalise these equations. There are two intrinsic scales, temperature $\sim \Delta T$ and lengths $\sim h$. We form velocity and time characteristic scales via *diffusive scaling*. From the thermal equation:

$$\frac{\Delta T}{t} \sim \frac{\Delta T U}{h} \sim \frac{\kappa \Delta T}{h^2}$$

From the second relation we have $U \sim \kappa/h$, then from the first we have $t \sim h^2/\kappa$. The non-dimensionalised equations (dropping $'$ henceforth) are

$$\begin{aligned} \nabla \cdot \boldsymbol{u} &= 0 \\ \frac{1}{\mathrm{Pr}} \frac{\partial \boldsymbol{u}}{\partial t} &= -\nabla p + \nabla^2 \boldsymbol{u} + \mathrm{Ra} T \hat{\boldsymbol{z}} \\ \frac{\partial T}{\partial t} - w &= \nabla^2 T \end{aligned} \tag{6}$$

where the *Prandtl number* $\mathrm{Pr} = \frac{\mu/\rho_0}{\kappa}$ which quantifies the importance of viscous diffusion versus thermal diffusion.

Boundary conditions. We require boundary conditions on the temperature T and velocity $\boldsymbol{u}$. There are several possible conditions, which may be mixed:

- Rigid boundary $[\boldsymbol{u} \cdot \hat{\boldsymbol{n}}]_{\text{boundary}} = 0$ where $\hat{\boldsymbol{n}}$ is outwards normal of boundary surface
- No-slip $[\boldsymbol{u} \times \hat{\boldsymbol{n}}]_{\text{boundary}} = 0$
- Stress-free (free slip) $\mu \frac{\partial u}{\partial n} = \mu \frac{\partial v}{\partial n} = 0$ i.e. $n = z$ in our picture
- Fixed temperature $T_{\text{boundary}} = \text{const.}$

- Fixed heat flux $[\hat{\boldsymbol{n}} \cdot \nabla T]_{\text{boundary}} = \text{const.}$

We eliminate pressure from the non-dimensionalised equations by taking $\hat{\boldsymbol{z}} \cdot \nabla \times (\nabla \times$ (6). Recall the vector identity

$$\nabla \times (\nabla \times \boldsymbol{A}) = \nabla(\nabla \cdot \boldsymbol{A}) - \nabla^2 \boldsymbol{A}$$

The governing equations are reduced to

$$\left(\mathrm{Pr}^{-1}\partial_t - \nabla^2\right)\nabla^2 w = \mathrm{Ra}\nabla_H^2 T \tag{7}$$

$$\left(\partial_t - \nabla^2\right) T = w \tag{8}$$

where $\nabla_H = (\partial_x, \partial_y, 0)$ is the horizontal gradient.

Normal modes. We examine growth/decay of perturbations of the form

$$(w, T) = (\hat{w}(z), \hat{T}(z))e^{i(kx+ly)+\sigma t}$$

For convenience, and given the x, y symmetry, define $a^2 = k^2 + l^2$ as an effective horizontal wavenumber. We have from the governing equations (7), (8):

$$\left[\sigma\mathrm{Pr}^{-1} - (D^2 - a^2)\right](D^2 - a^2) = -\mathrm{Ra}a^2\hat{T} \tag{9}$$

$$\left[\sigma - (D^2 - a^2)\right]\hat{T} = \hat{w} \tag{10}$$

where $D = \mathrm{d}/\mathrm{d}z$. The boundary in our case will be rigid, stress free, and fixed temperature. Note that this is not necessarily representative of the actual boundary conditions, but is useeful analytically. Thus at $z = 0, 1$ we have $w = 0$ (rigid), $D^2 w = 0$ (stress free) and $T = 0$ (fixed temperature). Given these conditions, the heat equation implies $D^2 T = 0$ on $z = 0, 1$ and the momentum equation implies $D^4 w = 0$ on $z = 0, 1$.

Marginal stability. The marginal stability boundary is $\sigma = 0$ between growth ($\sigma > 0$) and decay ($\sigma < 0$). Combining (9) and (10) with $\sigma = 0$ we hae

$$(D^2 - a^2)^3(\hat{T}, \hat{w}) = -a^2\mathrm{Ra}(\hat{T}, \hat{w})$$

The solutions have structure

$$(\hat{T}, \hat{w}) = (\hat{T}_0, \hat{w}_0)\sin n\pi z$$

Hence we have the eigenvalue condition $(n^2\pi^2 + a^2)^3 = a^2\mathrm{Ra}$. Let $a^2 = \pi^2 b^2$. Then

$$\mathrm{Ra} = \frac{(n^2 + b^2)^3\pi^4}{b^2}$$

The minimum Rayleigh number is at $n = 1$ where $\mathrm{Ra} = (1 + b^2)^3\pi^4/b^2$:

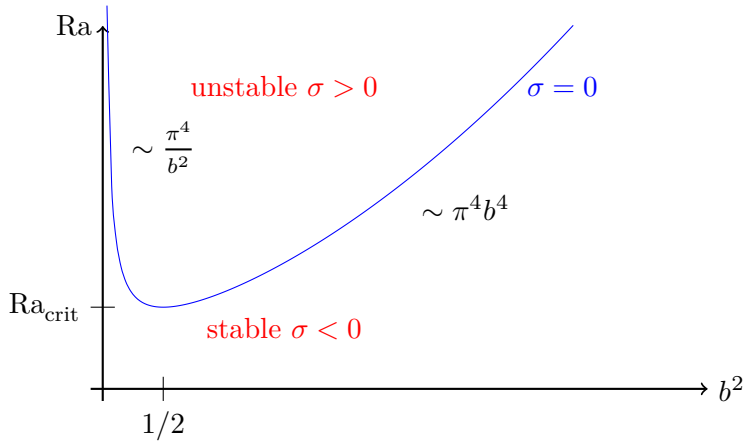

Setting $\partial \mathrm{Ra}/\partial b^2 = 0$ to find the critical Rayleigh number $\mathrm{Ra}_{\mathrm{crit}}$, we find

$$\mathrm{Ra}_{\mathrm{crit}} = \frac{27\pi^4}{4} \approx 657.5 \qquad \text{at } a = \frac{\pi}{\sqrt{2}}$$

Hence the dimensional wavelength at critical Rayleigh number is $2\pi h/a = 2\sqrt{2}h \approx 2.8h$. The convection process appears like so:

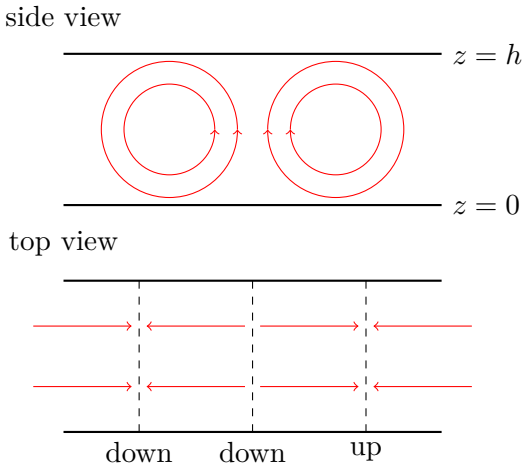

Example. Mantle convection. In the mantle, internal heating is due to radiogenic decay. We model this by adding a source term to the conservation of energy equation:

$$\rho_0 c_p \left(\frac{\partial T}{\partial t} + \boldsymbol{u} \cdot \nabla T \right) = \nabla \cdot (k \nabla T) + \rho_0 Q$$

where $Q = 10^{11} \mathrm{W kg}^{-1}$. The thermal boundary conditions are $T(0) = T_s$, i.e. fixed surface temperature, and $\partial T/\partial z = 0$ at $z = h$, i.e. zero basal heat flux.
A scaling analysis gives

$$x \sim h, \frac{k\Delta T}{h^2} \sim \rho_0 Q \implies \Delta T \sim \frac{\rho_0 Q h^2}{k}$$

The Rayleigh number in this case is

$$\mathrm{Ra}_Q = \frac{\rho_0 g \alpha (\rho_0 Q h^2/k) h^3}{\kappa \mu} = \frac{\rho_0^2 g \alpha Q h^5}{k \kappa \mu}$$

Typical values are $\mathrm{Ra}_Q = 3 \times 10^9$ and $\mathrm{Pr} = 10^{22}$. Note that Ra_Q is much larger than $\mathrm{Ra}_{\mathrm{crit}}$.

3.3 High Rayleigh number convection

At high Rayleigh number, the key idea is: small plumes are generated at boundaries, which only 'see' the statistically well-mixed interior temperature. Hence heat flux is independent of depth of domain.

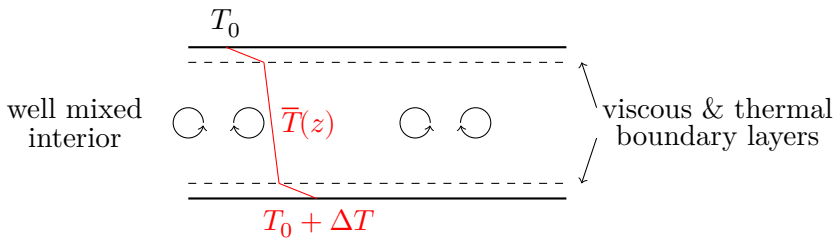

The heat flux is characterised by the *Nusselt number* defined by

$$\mathrm{Nu} = \frac{F_h}{k\Delta T/h} = f(\mathrm{Ra}, \mathrm{Pr})$$

where F_h is the heat flux, and Nu is a function of Ra, Pr only. If F_h is not a function of h, then we must have

$$F_h = \frac{k\Delta T}{h} f(\mathrm{Ra}, \mathrm{Pr}) \sim \frac{k\Delta T}{h} \mathrm{Ra}^{1/3}$$
$$\implies F_h = \lambda(\mathrm{Pr}) k \left(\frac{\rho_0 g \alpha}{K\mu}\right)^{1/3} \Delta T^{4/3}$$

for some function λ.

Boundary layer analysis. The picture was formalised by Lou Howard (1965). We assume the thermal boundary layer grows diffusively (i.e. slowly) according to

$$\frac{\partial T}{\partial t} = \kappa \frac{\partial^2 T}{\partial z^2}$$

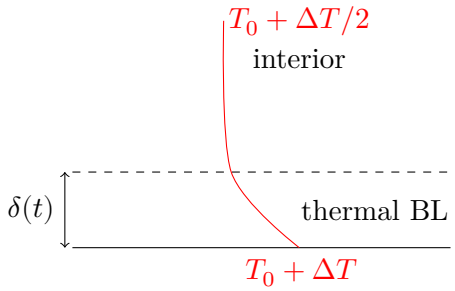

Diffusive scaling gives $z \sim \sqrt{\kappa t}$, i.e. a self-similar solution with similarity variable $\eta = z/2\sqrt{\kappa t}$. The thermal problem can be solved to get

$$T = T_0 + \frac{\Delta T}{2}\left[1 + \mathrm{erfc}(\frac{z}{2\sqrt{\kappa t}})\right]$$

The boundary layer is unstable when the local Rayleigh number exceeds the critical value.

$$\mathrm{Ra}_{BL} = \frac{\rho_0 g \alpha (\Delta T/2)\delta(t)^3}{\kappa\mu} \gtrapprox \mathrm{Ra}_{\mathrm{crit}}$$
$$\implies \frac{\delta}{h} \gtrapprox \left(\frac{2\mathrm{Ra}_c}{\mathrm{Ra}}\right)^{1/3}$$

Assume that advection of plumes from the boundary layer is fast compared with diffusive growth of the boundary layer. The heat flux is

$$F_h = \frac{k\Delta T}{2t_c}\int_0^{t_c}\frac{\mathrm{d}t}{\sqrt{\pi\kappa t}} = \frac{k\Delta T}{\delta_c}$$

Hence the Nusselt number can be written

$$\mathrm{Nu} = \frac{F_h}{k\Delta T/h} = \frac{h}{\delta_c} = \left(\frac{\mathrm{Ra}}{2\mathrm{Ra}_c}\right)^{1/3}$$

For $\mathrm{Ra}_{\mathrm{crit}} \approx 1100$, the Nusselt number is thus $\mathrm{Nu} \approx 0.077\mathrm{Ra}^{1/3}$ which matches well with experiment.

4 Solidification/melting

. Applications of solidification/melting theory include

- Formation of Earth's crust (early 1800s)
- Sea ice, due to Stefan (late 1800s)
- Earth's core (mid 1950s)
- Igneous rocks (mid 1980s)

4.1 The Stefan condition

Consider a solid–liquid interface $x = a(t)$ with boundary velocity v_n. We will work in the frame of reference moving with the boundary.

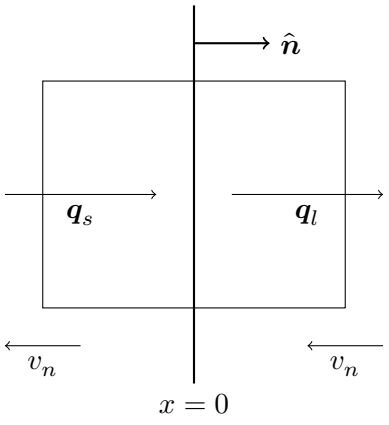

We assume there is a heat flux $\boldsymbol{q}_s$ into the control volume, and a heat flux $\boldsymbol{q}_l$ leaving the control volume. Assume equal densities for the liquid and solid, i.e. $\rho_l = \rho_s = \rho$. Conservation of energy in the control volume gives:

$$\rho H_l v_n - \hat{\boldsymbol{n}}\cdot\boldsymbol{q}_l - \rho H_s v_n + \hat{\boldsymbol{n}}\cdot\boldsymbol{q}_s = 0$$

where $\boldsymbol{q} = -k\nabla T$ and H is the *specific enthalpy*, which is the heat energy at constant pressure per unit mass. Rearranging, we have

$$\rho(H_l - H_s)v_n = \hat{\boldsymbol{n}}\cdot(\boldsymbol{q}_l - \boldsymbol{q}_s)$$

Define $L = H_l - H_s = T_m(s_s - s_l)$ where T_m is the melting temperature and s is the entropy of solid/liquid. L is the latent heat of fusion/solidification. At the boundary $x = a(t)$ we have

$$\rho L v_n = k\hat{\boldsymbol{n}} \cdot (\nabla T|_s - \nabla T|_l)$$

where all quantities are evaluated at the boundary. This is the *Stefan condition*.
Note that if $\rho_s \neq \rho_l$ there is a velocity u_n induced at the interface:

$$u_n = \frac{\rho_l - \rho_s}{\rho_l} v_n$$

in which case the Stefan condition is modified to

$$\rho_s L v_n = k_s \hat{\boldsymbol{n}} \cdot \nabla T|_s - k_l \hat{\boldsymbol{n}} \cdot \nabla T|_l$$

4.2 1D solification from a cooled boundary

For convenience we again assume equal densities and thermal properties.

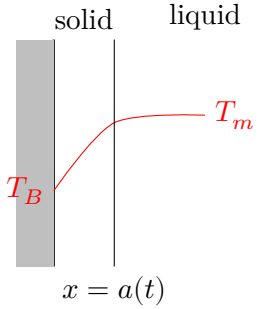

In the solid, the temperature T obeys

$$\frac{\partial T}{\partial t} = \kappa \frac{\partial^2 T}{\partial x^2}$$

with boundary conditions $T = T_B$ at $x = 0$ and $T = T_m$ at $x = a(t)$. We also have the Stefan condition

$$\rho L \dot{a} = k \left.\frac{\partial T}{\partial x}\right|_{a^-}$$

at $x = a(t)$.
Scaling from the thermal equation gives $x \sim \sqrt{\kappa t}$ as usual. From Stefan's condition we have

$$\rho L \frac{x}{t} \sim k \frac{\Delta T}{x} = \rho c_p \kappa \frac{\Delta T}{x}$$

which yields $x \sim \sqrt{\kappa t \frac{c_p \Delta T}{L}}$. The factor in the square root is dimensionless, hence we have $x \sim \sqrt{\kappa t}$ in agreement with the thermal equation. We use similarity variable $\eta = x/2\sqrt{\kappa t}$ and define $\theta(\eta)$ via

$$T - T_B = (T_m - T_B)\theta(\eta)$$

Now $a(t) = 2\lambda\sqrt{\kappa t}$, thus the diffusion equation becomes

$$-2\eta\theta' = \theta''$$

with $0 \leq \theta \leq \lambda$. The boundary conditions are now $\theta(0) = 0, \theta(1) = \lambda$ and

$$2\mathcal{S}\lambda = \theta'(\lambda)$$

where $\mathcal{S} = L/c_p\Delta T$ is the Stefan number. The solution is

$$\theta = \frac{\operatorname{erf}\eta}{\operatorname{erf}\lambda}$$

where λ satisfies

$$\sqrt{\pi}\lambda e^{\lambda^2}\operatorname{erf}\lambda = \frac{1}{\mathcal{S}}$$

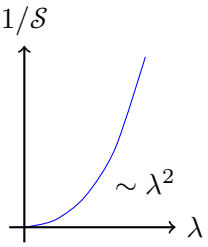

Large $\mathcal{S}$ implies small λ, i.e. small growth, and vice versa. Note for water, $L/c_p \approx 80°\text{C}$.

4.2.1 Quasi-steady approximation

When $\mathcal{S} \gg 1$ the Stefan condition implies growth is slow. Rescale time $t \to \mathcal{S}t$ so the time derivative becomes $\mathcal{O}(\mathcal{S}^{-1})$. Then

$$\frac{\partial^2 T}{\partial x^2} \approx 0 \implies \frac{\partial T}{\partial x} = \frac{T_m - T_B}{a}$$

i.e. there is a linear conduction profile in the solid. The Stefan condition is now

$$\rho L\dot{a} = k\left.\frac{\partial T}{\partial x}\right|_a \approx \frac{k(T_m - T_B)}{a}$$

where $a = \sqrt{2\kappa t/\mathcal{S}}$. This definition of a follows from: $\mathcal{S} \gg 1 \implies \lambda \ll 1$. Then

$$\sqrt{\pi}\lambda e^{\lambda^2}\operatorname{erf}\lambda = \frac{1}{\mathcal{S}} \approx \sqrt{\pi}\lambda \cdot 1 \cdot \frac{2}{\sqrt{\pi}}\lambda$$

Hence $\lambda \sim (1/2\mathcal{S})^{1/2}$, from which $a(t) = 2\lambda\sqrt{\kappa t}$ gives a as above.
Note: as $t \to 0$, $\dot{a} \sim t^{-1/2} \to \infty$. This is physically implausible; in fact growth is regularised by crystal kinetics which is not included in this model.

4.3 Phase change and fluid flow

Consider 2D stagnation point flow driving a steady melting of a solid, with fluid velocity

$$\boldsymbol{u} = (Ex, -Ez)$$

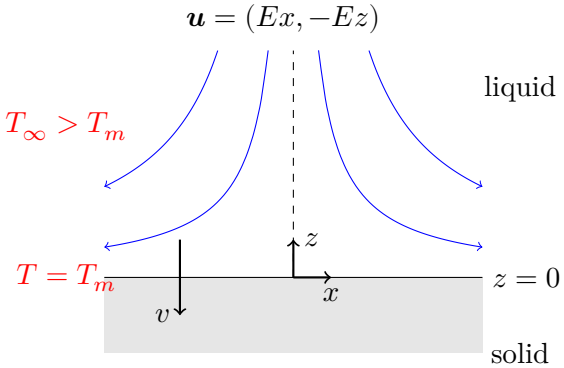

Steady-state in a translating frame of reference (i.e. moving with boundary at speed v) implies $T = T(z)$ is a function of z only. In steady-state are left with a balance of advection and diffusion:

$$(v - Ez)\frac{\partial T}{\partial z} = \kappa \frac{\partial^2 T}{\partial z^2}$$

where v is the melt rate. Neglecting advection by the frame (justify later) we have solution

$$T = T_m + (T_\infty - T_m)\,\mathrm{erf}\left(\sqrt{\frac{E}{2\kappa}}z\right)$$

The Stefan condition gives

$$-\rho L v = -k\left.\frac{\partial T}{\partial z}\right|_{z=0} = -k\frac{2}{\sqrt{\pi}}(T_\infty - T_m)\sqrt{\frac{E}{2\kappa}}$$

Hence the melt rate can be written as

$$v = \frac{1}{\mathcal{S}}\sqrt{\frac{2E\kappa}{\pi}}$$

Note the following:

- The melt rate v increases as flow rate E increases ($v \sim \sqrt{E}$)
- The thermal boundary layer has scale $\delta_T \sim \sqrt{\kappa/E}$. Thus δ_T decreases as E increases, i.e. the flow compresses the thermal boundary layer
- The ratio of frame advection to flow compression is

  $$\frac{\text{advection}}{\text{compression}} \sim \frac{v}{Ez} \sim \frac{v}{E\delta T} \sim \frac{v}{\sqrt{E\kappa}} \sim \frac{1}{\mathcal{S}}$$

  So neglect of frame advection is valid if $\mathcal{S} \gg 1$.

4.4 Solidification with vigorous convection

Consider solidification of a liquid with vigorous convection, so that there is a well-mixed interior temperature $\overline{T}(t)$ in the liquid.

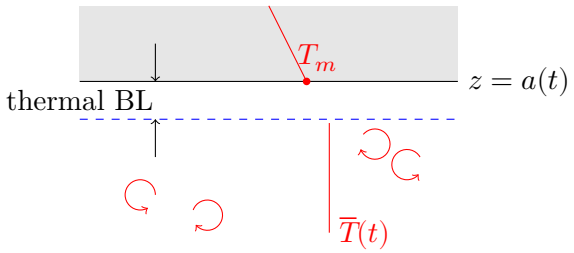

Recall from earlier sections that high Rayleigh number convection has heat flux

$$F_T = \lambda k\left(\frac{\rho_0 g\alpha}{\kappa\mu}\right)^{1/3}(\overline{T} - T_m)^{4/3}$$

Consider a control volume around the solid–liquid interface *and* the thermal boundary layer, and impose energy conservation. Note that the control volume is in a frame of reference moving at the melt rate v with the interface.

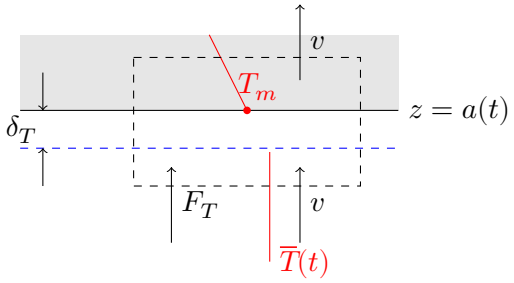

Conservation of energy with melt rate v gives

$$\rho(H_l - H_s)v + \rho c_p(\overline{T} - T_m)v + F_T - k\left.\frac{\partial T}{\partial z}\right|_{a^-} = 0$$

Rearranging, we have

$$\rho\left[L + c_p(\overline{T} - T_m)\right]v = k\left.\frac{\partial T}{\partial z}\right|_{a^-} - F_T$$

The first term is the release of latent heat, the second is cooling across the boundary layer, the third is conduction in the solid and the final term is the convective heat flux. This is the modified Stefan condition (needed for ES1 Q4).

4.5 Earth's core

Consider solidification of the Earth's inner core, driven by heat flux F_m from the mantle.

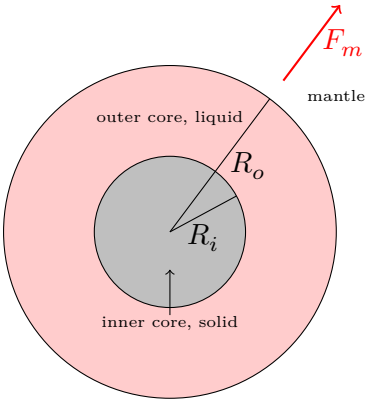

We require a relation between the melt temperature $T_m = T_m(p)$ and the pressure p, which is provided by the *Clausius-Clapeyron equation*:

$$\rho_s \frac{L}{T_m}\frac{\partial T_m}{\partial p} = \frac{\rho_s}{\rho_l} - 1$$

The RHS quantity is position for iron in the inner core. To leading order, the pressure is hydrostatic

$$\frac{\partial p}{\partial r} = -\rho g(r) = -\rho\frac{G}{r^2}\left(\frac{4\pi}{3}r^3\rho\right) = -\frac{4\pi}{3}G\rho^2 r$$

$$\implies p = p_0 - \frac{2\pi}{3}G\rho^2 r^2$$

Substituting this form of the pressure into the Clausius-Clapeyron equation gives

$$T_m \approx T_0 - \frac{2\pi}{3}\frac{GT_0(\rho_s - \rho_l)}{L}r^2$$

The radius at which the core temperature T is larger than T_m is where the solid–liquid interface exists, i.e. at $r = R_i$.

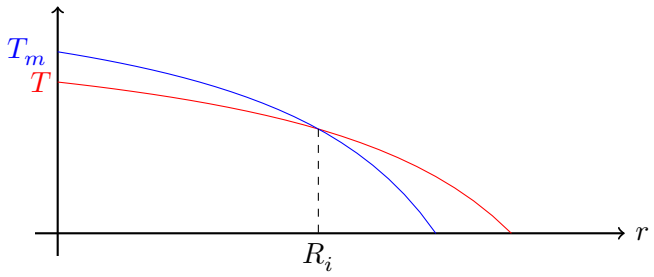

Consider the two choices of limiting cases:

1. No heat flux from inner core
2. Perfectly conducting inner core $T_{IC} = T_m$. Outer core is convecting vigorously so assume well mixed, T is adiabatic, i.e. 'potential temperature' is isothermal.

The balance of heat fluxes is

$$4\pi R_0^2 F_m = \frac{4\pi}{3}\left[R_0^3 - R_i^3\right]\rho c_p \frac{\partial T_m}{\partial t} + \rho L 4\pi R_i^2 \frac{\mathrm{d}R_i}{\mathrm{d}t}$$

In case (ii) the R_i^3 term in the first RHS term is neglected. In this case,

$$4\pi R_0^2 F_m = \frac{4\pi}{3} R_0^3 \rho c_p \cdot \frac{4\pi}{3}\frac{G T_m \delta\rho}{L} R_i \dot{R}_i + \rho L 4\pi R_i^2 \dot{R}_i$$

Hence the time averaged mantle heat flux is

$$\frac{1}{m}\int_0^t F_m(t')\,\mathrm{d}t' = \zeta^2 + \mathcal{S}\zeta^3$$

where $\zeta = R_i/R_o$, the Stefan number is $\mathcal{S} = \rho L R_o/m$ and

$$m = \frac{2}{9} R_0^3 \rho c_p \frac{G T_m \delta\rho}{L}$$

Real-world measurements give $\zeta = 1/3, \mathcal{S} = 0.4$, so growth is controlled by the mantle heat flux balancing cooling (rather than latent heat). Note that knowing $\zeta = 1/3$ does not allow a good estimate of the age of the inner core, given the upper and lower bounds:

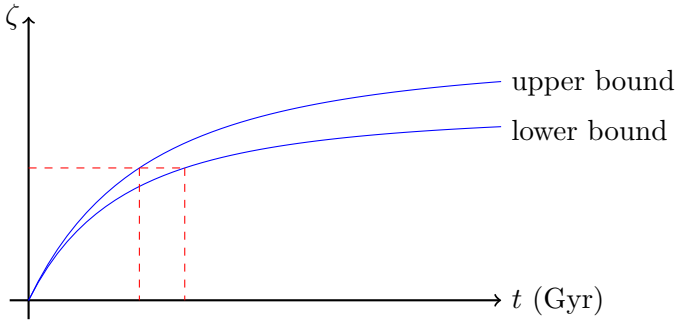

5 Flows in porous media

To avoid the complexity of modelling very fine details, we model the flow averaged over many *pore scales* and assume viscous dissipation balances the driving forces.

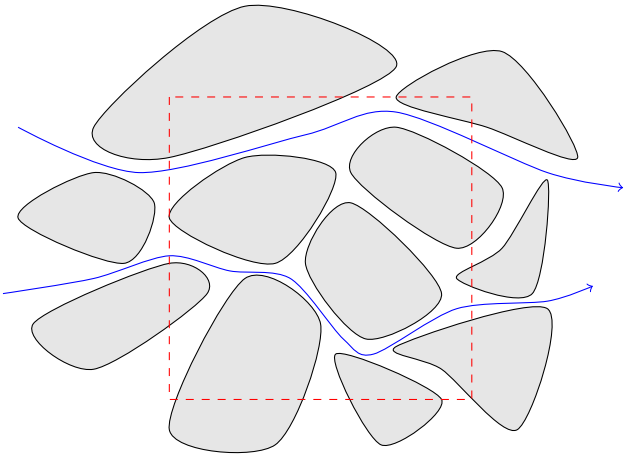

Define the *porosity*

$$\phi = \frac{\text{fluid volume}}{\text{total volume}}$$

so that tightly packed media has low porosity and highly saturated media has high porosity. For context, random close-packed spheres have $\phi \approx 0.37$ whilst hexagonally close-packed monodisperse spheres have $\phi = 1 - \pi/3\sqrt{2} \approx 0.26$.

5.1 Darcy's law

Darcy's law represents the assumption that viscous dissipation at the pore scale balances the driving forces, pressure and buoyancy. We have

$$\mu \frac{\boldsymbol{u}}{K(\phi)} = -(\nabla p + \rho g \hat{\boldsymbol{z}})$$

where $\boldsymbol{u} = \phi \tilde{\boldsymbol{u}}$ is the fluid flux per unit area and $\tilde{\boldsymbol{u}}$ is the *interstitial fluid velocity*, i.e. the actual fluid velocity. The tensor $K(\phi)$ is the *permeability*, which characterises the resistance to flow. In general, this is a tensor and depends on local properties. K reflects the geometry/tortuosity and porosity of the medium.

Example. The Kozeny-Carman equation for monodisperse random close packed spheres gives

$$K = \frac{d^2}{180} \frac{\phi^3}{(1-\phi)^2}$$

where d is the grain size.

5.2 Porous gravity currents

Consider flows in a confined aquifer: we assume two fluids with density $\rho + \Delta\rho$ and ρ separated by an interface $z = h(x,t)$ with the nose of the gravity current at $x = x_N(t)$ in an aquifer of height H. There is a volume flux Q injected into the aquifer and background pressure $p_0(x,z,t)$.

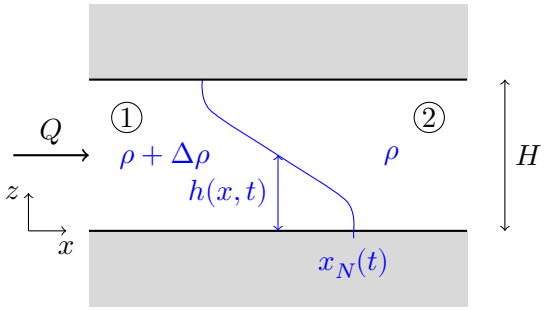

The large aspect ratio implies the flow is mainly horizontal, hence pressure is hydrostatic to leading order. The flow is driven by a combination of buoyancy ($\sim \Delta\rho g$) and injection ($\sim Q$), and is primarily horizontal. The pressure in the injected (lower) fluid is

$$p_1 = p_0 - (\rho + \Delta\rho)gz$$

whilst the pressure in the ambient (upper) fluid) is

$$p_2 = p_0 - (\rho + \Delta\rho)gh - \rho g(z - h)$$

The fluid flow is given by Darcy's law. For the injected fluid,

$$u_1 = -\frac{k}{\mu}\frac{\partial p_1}{\partial x} = -\frac{k}{\mu}\frac{\partial p_0}{\partial x}$$

Similarly, for the ambient fluid

$$u_2 = -\frac{k}{\mu}\frac{\partial p_2}{\partial x} = -\frac{k}{\mu}\left(\frac{\partial p_0}{\partial x} - \Delta\rho g\frac{\partial h}{\partial x}\right)$$

Now global conservation of the fluid flux gives

$$Q = u_1 h + u_2(H - h) = -\frac{k}{\mu}\left[\frac{\partial p_0}{\partial x}h + \frac{\partial p_0}{\partial x}(H - h) - \Delta\rho g\frac{\partial h}{\partial x}(H - h)\right]$$

Rearranging for the background pressure gradient gives the injected fluid velocity as

$$u_1 = -\frac{k}{\mu}\frac{\partial p_0}{\partial x} = \frac{Q}{H} - \frac{k\Delta\rho g}{\mu}\frac{H - h}{H}\frac{\partial h}{\partial x}$$

Local mass conservation in the lower (injected) layer gives

$$\begin{aligned} &\phi\frac{\partial h}{\partial t} + \frac{\partial}{\partial x}(u_1 h) = 0 \\ \implies &\phi\frac{\partial h}{\partial t} + \frac{\partial}{\partial x}(\frac{Qh}{H}) = \frac{k\Delta\rho g}{\mu}\frac{\partial}{\partial x}\left[\frac{H - h}{H}h\frac{\partial h}{\partial x}\right] \end{aligned}$$

The first term is the change in fluid mass, the second the injection pressure driven flux, and the RHS term is the buoyancy driven flux.